Biophysical Chemistry 168-169 (2012) 40–47

Contents lists available at SciVerse ScienceDirect

Biophysical Chemistry

journal homepage: http://www.elsevier.com/locate/biophyschem

Importance of polypeptide chain length for the correct local folding of a β-sheet protein

Mio Yamamoto, Kanako Nakagawa [1], Masamichi Ikeguchi *

Department of Bioinformatics, Soka University, 1-236 Tangi-cho, Hachioji, Tokyo 192-8577, Japan

HIGHLIGHTS

- ► An α-helix is converted into a β-structure during equine β-lactoglobulin folding.
- ► This α → β transition can be induced by the unstructured polypeptide chain.
- ► The longer the chain, the more stable the β-structure.

GRAPHICAL ABSTRACT

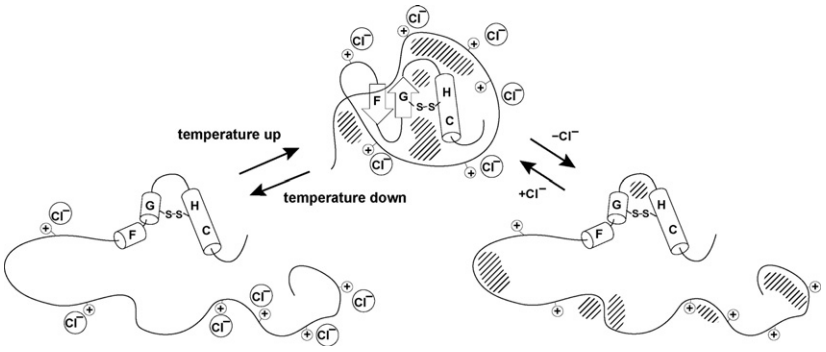

ARTICLE INFO

Article history:
Received 21 April 2012
Received in revised form 10 June 2012
Accepted 17 June 2012
Available online 23 June 2012

Keywords:
α → β Transition
β-Hairpin
Circular dichroism
Non-native α-helix
8-Anilino-1-napthalenesulfonic acid
Molten globule

ABSTRACT

Equine β-lactoglobulin is a 162-residue β-sheet protein. A partially folded form of equine β-lactoglobulin contains a β-hairpin and an α-helix. The β-hairpin converts into non-native α-helices at temperatures <0 °C. CHIBL, a truncated equine β-lactoglobulin (residues 88–142), contains the low-temperature α-helical structure even at room temperature, indicating that the interactions responsible for the stability of the β-hairpin reside in non-CHIBL residues. For the study reported herein, we characterized two truncated mutants and their leucine103 → proline103 variants to identify residues that stabilize the β-hairpin. The dependence of their circular dichroism spectra on chloride ion concentration and temperature revealed that the ability to transition from the non-native α-helices to the β-hairpin depends on the polypeptide chain length and improves as the chain length increases despite the apparent absence of any ordered structure in the extended sequences.

1. Introduction

The inherent propensities of individual amino acid residues within peptides and proteins to form particular types of secondary structures, e.g., α-helices and β-sheets, vary according to the chemical and conformational characteristics of the amino acids [1]. The frequency of an amino acid in a given type of secondary structure depends, in part, on its inherent propensity. However, accurate prediction of secondary structures using only the inherent propensities of amino acids is difficult because secondary structure formation is also affected by context-dependent effects, i.e., non-local interactions. For example, the secondary structure of the 11-residue chameleon sequence depends on its location within the sequence of the IgG-binding domain of protein G, indicating that its secondary structure is determined by tertiary interactions [2]. As a second example, α-helix → β-sheet (α → β) transitions occur during the folding of certain proteins, e.g., β-lactoglobulin [3,4] and SH3 domains [5], indicating that the secondary structures of

* Corresponding author. Tel.: +81 42 691 9444; fax: +81 42 691 9312.
E-mail address: ikeguchi@soka.ac.jp (M. Ikeguchi).
[1] New Industry Creation Hatchery Center, Tohoku University, 6-6-10 Aoba, Aramaki, Aoba-ku, Sendai 980-8579, Japan.

0301-4622/$ – see front matter © 2012 Elsevier B.V. All rights reserved.
doi:10.1016/j.bpc.2012.06.002

those sequences are determined by the inherent propensities of their residues at early stages of folding and by context at later stages. For the study reported herein, we characterized factors that affect the α → β transition in analogs of equine β-lactoglobulin (ELG) folding intermediates.

ELG is a major whey protein of 162 residues and has two disulfide bonds (Cys66 − Cys160 and Cys106–Cys119), an eight-strand (strands A–H) antiparallel β-barrel, an α-helix in its C-terminal region, (C-terminal α-helix), and an off-barrel β-strand (strand I), also in the C-terminal region [6]. Its acid-denatured (A) state (Fig. 1A) is a partially folded, compact globular structure with a native-like β-hairpin and a nonnative α-helix [7,8]. The A state and the ELG burst-phase folding intermediate appear to be identical, or nearly identical, in structure [4]. The A and native states of ELG also undergo similar cold denaturation, resulting in expanded, chain-like conformations containing additional nonnative helices (the C state, Fig. 1B) [9]. This suggests that the structure in the A state is stabilized by hydrophobic interactions, because cold denaturation results from the preferential hydration of nonpolar groups at low temperature [10].

The native structure of a mutant ELG (C66A/C160A), in which Cys66 and Cys160 are replaced with alanines, is similar to that of native ELG [11]. Under acidic and high salt conditions (0.1 M HCl/KCl, pH 1.5), C66A/C160A assumes a structure similar to that of the ELG A state (Fig. 1D) [11]. However under low salt and acidic conditions (0.1 M H_3PO_4, pH 1.7), C66A/C160A assumes a conformation similar to the C state of wild-type ELG (Fig. 1F) [12], whereas wild-type ELG maintains the A-state conformation under the aforementioned conditions (Fig. 1C). Notably, Goto and coworkers found that the A states of apomyoglobin and cytochrome *c* are stabilized in acid by anion-induced reduction of electrostatic repulsions between positively charged residues [13]. Furthermore, they showed that the effectiveness of anions for A state stabilization varies with the type of anion [13]. Given the behavior of C66A/C160A, Cl^- (0.1 M HCl/KCl, pH 1.5) probably decreases the electrostatic repulsion so as to maintain the A state in acid, although the equivalent concentration of H_3PO_4 cannot do so because only 38% of the acid is dissociated and phosphate ion is not as effective as Cl^- [11,12]. Additionally, even in the presence of 0.1 M Cl^-, the A state (Fig. 1D) of C66A/C160A is transformed into the C state at lower temperatures (Fig. 1E) [14]. Therefore, electrostatic repulsion or attenuation of the hydrophobic effect at low temperatures causes the C66A/C160A chain to expand (summarized in Fig. 1).

The secondary structures present in the A and C states have been characterized using hydrogen exchange [6] and proline-scanning mutagenesis [8]. In the A state, a β-hairpin in the sequence containing the F and G strands is present. Conversely, the same regions form nonnative helices in the C state. In both states, the H-strand sequence adopts a non-native helix, and it is merged with the native C-terminal α-helix forming one long helix [15]. Therefore, the anion- or temperature-induced compaction of the chain is responsible for the α → β transitions in the F- and G-strand region.

An ELG fragment (residues 88–142) that includes the sequences for the F, G, and H strands, and the C-terminal helix (denoted CHIBL, Fig. 2) has a structure under all ionic strength and temperature conditions (see below and Ref. [14]) similar to that found for the C state of C66A/C160A, indicating that residues outside CHIBL are necessary for the α → β transitions of strands F and G.

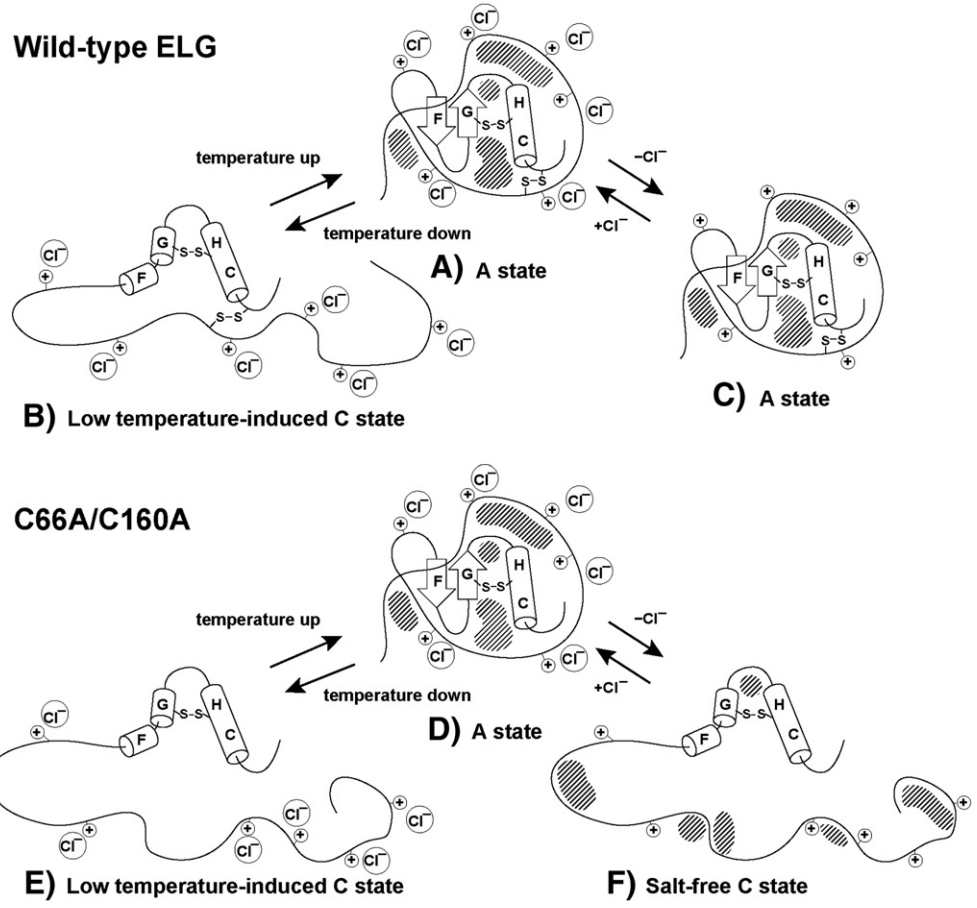

Fig. 1. Schematic of the A- and C-state transitions in wild-type ELG (A, B, C) and C66A/C160A (D, E, F). The β-strands and α-helices are shown as arrows and cylinders, respectively. The sequences containing the native F and G β-strands are labeled F and G, respectively. The H β-strand and the C-terminal helix found in the native conformation are shown as a long non-native helix, labeled HC. Hatched areas represent hydrophobic environments. Positively charged residues and Cl^- anions are labeled with a plus sign and as Cl^-, respectively. The secondary structures of wild-type ELG are assumed to be similar to those of C66A/C160A.

Fig. 2. Schematics of the CHIBL, 60–162, 30–162, and 1–162 sequences. Residue numbers correspond to those of ELG. The 20-residue, N-terminal tags are indicated by broken lines. The sequences that adopt secondary structures in native ELG are shown at the top of the figure (strands A–I and the C-terminal helix).

For the study reported herein, we characterized truncated forms of C66A/C160A that contain residues 30–162 or 60–162 (Fig. 2) to identify residues that stabilize the β-hairpin in the A state. The formation of the β-hairpin in the F- and G-strand region was assessed, using circular dichroism (CD) spectroscopy, by answering the following questions. (i) Do the conformations of the mutants undergo a temperature-dependent change that is cooperative (sigmoidal shaped) as has been observed for C66A/C160A [14]? (ii) Does Cl^- affect their conformations under acid conditions? (iii) Does a Leu103 → Pro substitution (in the G-strand sequence) cause a conformational change, as has been observed for C66A/C160A?

2. Material and methods

2.1. Truncation mutants

The N-terminal truncated C66A/C160A mutants 30–162 and 60–162 and the C-terminal truncated mutant 1–87 were constructed by PCR with suitable primers and the plasmid containing the C66A/C160A gene as the template [11]. The proline mutants 30–162_L103P and 60–162_L103P were constructed by site-directed mutagenesis using QuikChange kit reagents (Stratagene). DNA sequencing used an ABI PRISM 3100-Avant sequencer to confirm the sequences of the mutant genes. After sequence confirmation, the genes were individually inserted into pET 15b vectors, which were then separately transformed into *Escherichia coli* BL21 (DE3) samples. Similarly, the genes of C66A/C160A and its corresponding L103P mutant [8] were also transferred from pET 3c to pET 15b, so that all expressed proteins in this study contain the 20-residue N-terminal tag including hexahistidine.

2.2. Expression, refolding, and purification of deletion mutants

Proteins were expressed, refolded, and purified as described for CHIBLΔF, a truncated CHIBL sequence [15]. The purities of the proteins were confirmed by sodium dodecyl sulfate-polyacrylamide gel electrophoresis and analytical reverse-phase high performance liquid chromatography.

2.3. CD spectroscopy

CD spectra were recorded using Jasco J-720 and Applied Photophysics Chirascan spectropolarimeters. Unless otherwise indicated, protein concentration, as determined by ultraviolet spectroscopy, was 0.2 mg/mL. The extinction coefficients for the truncated mutants were calculated using the extinction coefficients of tyrosine ($1280\,M^{-1}cm^{-1}$) and tryptophan ($5690\,M^{-1}cm^{-1}$) [16]. An extinction coefficient of $12{,}000\,M^{-1}cm^{-1}$ was used for 1–162 and C66A/C160A [7]. Cuvettes with path lengths between 1 and 10 mm were used. The dependence of the CD on temperatures below 0 °C was monitored using supercooled solutions.

2.4. Sedimentation velocity

Sedimentation velocity experiments were performed using a Beckman XL-I analytical ultracentrifuge and an An-50 Ti rotor at 20 °C at 40,000 rpm. The solution condition was 0.1 M HCl/KCl (pH 1.7). Sedimentation of the proteins was monitored at 220–230 nm and 1-min intervals using a radial-step size of 0.003 cm. Protein concentrations were 0.05–0.35 mg/mL. Data were analyzed with SEDFIT 12.1 [17].

2.5. Fluorescence spectroscopy

8-Anilino-1-napthalenesulfonic acid (ANS) fluorescence spectra were recorded using a Jasco FP-6500 spectrofluorometer. The concentration of ANS was determined from measurements of ultraviolet absorbance, using an extinction coefficient of $7800\,M^{-1}cm^{-1}$ at 372 nm [18]. The protein and ANS concentrations were 2 μM and 10 μM, respectively. The samples were excited at 372 nm (band width 3 nm) and emission spectra were recorded from 400 nm to 600 nm with a band width 5 nm.

3. Results

3.1. The N-terminal tag does not affect the conformation of 1–162

All truncated mutants used in this study contained a 20-residue N-terminal tag to facilitate purification. To assess the effect of the tag on the conformations of the mutants, we constructed 1–162, which is a tagged C66A/C160A. We then compared the conformational properties of 1–162 and C66A/C160A. The CD spectra of 1–162 and C66A/C160A in 0.1 M H_3PO_4 or in 0.1 M HCl/KCl [11] are almost identical (Fig. S1). Under acidic conditions, the CD spectra of both proteins are similarly affected by Cl^- concentration. The mean residue ellipticity ($[\theta]_{MRE\ 222}$) of 1–162 at 222 nm in 0.1 M H_3PO_4 is more negative than it is for 1–162 in 0.1 M HCl/KCl (Fig. 3A). The CD spectrum of 1–162 in the absence and presence of Cl^- is independent of protein concentration between 0.05 and 0.5 mg/mL (data not shown). For this concentration range, the sedimentation coefficient of 1–162 in 0.1 M HCl/KCl is 1.6 S, which corresponds to a hydrodynamic radius of 30.1 Å (Fig. S2) and is a smaller value than that found for wild-type ELG in the C state (37.1 Å) [9] or for that expected for an unfolded protein of the same length (42.9 Å) [19]. Therefore, at a concentration of ~0.5 mg/mL, 1–162 appears to be a compact monomer. The temperature dependence of $[\theta]_{MRE\ 222}$ for 1–162 in the absence and presence of 0.1 M Cl^- is shown in Fig. 3B. $[\theta]_{MRE\ 222}$ decreases linearly with decreasing temperature in the absence of Cl^-. A similar temperature dependence was observed for CHIBL and CHIBLΔF $[\theta]_{MRE\ 222}$ values [15]. A recent NMR study showed that the population of the helical conformation in CHIBLΔF is ~50% at 12 °C and suggested that the temperature-dependent decrease in $[\theta]_{MRE}$ reflects the increase in the population of helical conformation [15]. Therefore, the linear change in $[\theta]_{MRE\ 222}$ (Fig. 3B) probably indicates that the helical population in the region corresponding to CHIBL increases, whereas other regions remain unstructured. In 0.1 M Cl^-, however, the change in $[\theta]_{MRE\ 222}$ as a function of temperature has a slightly sigmoidal shape, and its value coincides with that for low Cl^- and low temperature conditions. The same effects induced by temperature and Cl^- concentration were also observed for C66A/C160A [14].

A proline was substituted for L103 in the G strand of 1–162 to assess its effect on the conformation of the F- and G-strand region because a proline that replaces a residue residing in a secondary structure is expected to disrupt that secondary structure [8]. A difference CD spectrum can report if a disrupted secondary structure is an α-helix or β-sheet [8]. The L103 → P substitution significantly reduces the $[\theta]_{MRE\ 222}$ of 1–162 in the presence and absence of Cl^- (Fig. S3). If the secondary structure(s) in the F- and G-strand region are altered by temperature, the difference spectra at both temperatures (25 °C and −5 °C) for 1–162 and 1–162_L103P ($\Delta[\theta]_\lambda = [\theta]_{\lambda\ 1-162} - [\theta]_{\lambda\ 1-162\_L103P}$) should

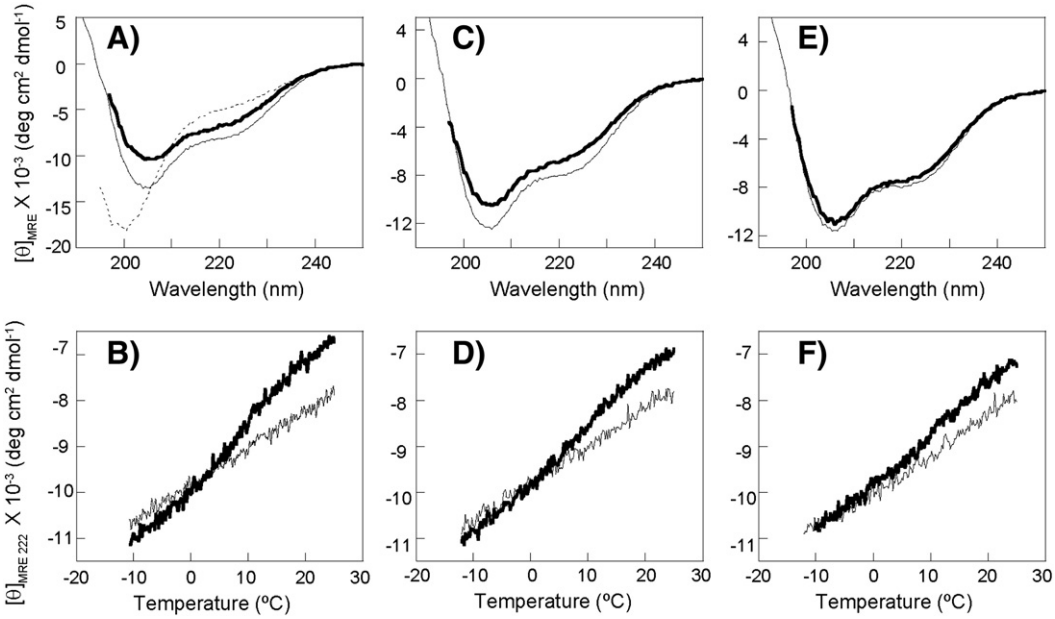

Fig. 3. CD spectra of 1–162, 30–162, and 60–162. The CD spectra of (A) 1–162, (C) 30–162, and (E) 60–162 in 0.1 M H_3PO_4 (thin lines) or in 0.1 M HCl/KCl (thick lines) at pH 1.7 and 25 °C. The dotted line in (A) is CD spectrum of 1–87 in 0.1 M H_3PO_4. The temperature dependence of the $[\theta]_{MRE\ 222}$ for (B) 1–162, (D) 30–162, and (F) 60–162 in 0.1 M H_3PO_4 (thin lines) or 0.1 M HCl/KCl (thick lines) at pH 1.7.

differ. In the absence of Cl^-, the difference spectra have negative peaks at 222 and 208 nm at both temperatures (Fig. 4A), indicating that 1–162 contains α-helices at both temperatures. In contrast, in the presence of Cl^-, the shapes of the difference spectra are not the same at 25 °C and −5 °C (Fig. 4B). At −5 °C, the shape of the difference spectrum is similar to that obtained in the absence of Cl^-. At 25 °C, however, the difference spectrum has a very weak negative peak at 215 nm, indicating a β-sheet-type conformation. The conformation of the F- and G-strand region in 0.1 M HCl/KCl therefore probably changes from an α-helix to a β-hairpin when the temperature increased, as was shown for C66A/C160A [14]. Because the transitions found for 1–162 and C66A/C160A under all tested conditions are the same, the tag does not seem to affect the conformational properties of C66A/C160A.

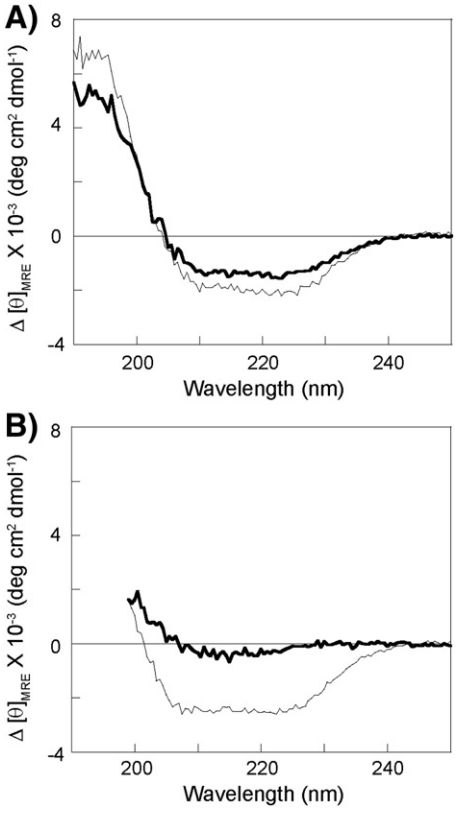

Fig. 4. Difference CD spectra ($[\theta]_{\lambda\ 1-162} - [\theta]_{\lambda\ 1-162\_L103P}$) for 1–162 and 1–162_L103P. (A) 0.1 M H_3PO_4 (B) 0.1 M HCl/KCl each at 25 °C (thick lines) or −5 °C (thin lines) and pH 1.7.

3.2. Dependency of local secondary structures on polypeptide chain length

To identify non-local residues that might contribute to β-hairpin stabilization in the F- and G-strand region, we constructed the deletion mutants 30–162 and 60–162. Fig. 3C and E show the CD spectra for 30–162 and 60–162, respectively, in the absence and presence of 0.1 M Cl^- at pH 1.7. The CD spectra of both mutants do not depend on protein concentration between 0.05 and 0.5 mg/mL in the absence or presence of Cl^- (data not shown). In this range of protein concentration, the sedimentation coefficients for 30–162 and 60–162 in 0.1 M HCl/KCl are 1.5 and 1.4 S, respectively (Fig. S2), corresponding to hydrodynamic radii of 27.9 and 24.2 Å, respectively. These values are smaller than that expected for unfolded proteins of the same lengths (for 30–162, 38.9 Å and for 60–162 34.3 Å [19]), indicating that both mutants are monomeric at <0.5 mg/mL. In the absence of Cl^-, the $[\theta]_{MRE\ 222}$ for 30–162 was noticeably more negative from that obtained in the presence of Cl^- (Fig. 3C), whereas the difference in the $[\theta]_{MRE\ 222}$ values for 60–162, although trending in the same direction, was slight (Fig. 3E). In summary the difference in $[\theta]_{MRE\ 222}$ in the absence and presence of Cl^- was largest for 1–162 and decreased as the polypeptide chain length decreased (Fig. 5A). Notably, the CD spectrum of CHIBL does not depend on the Cl^- concentration [14]. In the presence of 0.1 M Cl^-, the $[\theta]_{MRE\ 222}$ values for 30–162 and 60–162 (Fig. 3D and F, respectively) decrease sigmoidally as the temperature decreases. Conversely, in the absence of Cl^-, the $[\theta]_{MRE\ 222}$ values for 30–162 and 60–162 decrease linearly with decreasing temperature, and reach similar values as those obtained for 0.1 M Cl^- at temperatures below −5 °C. By reporting the temperature dependence of the CD using the molar ellipticity ($[\theta]_M$) scale, a direct comparison of the change in ellipticity for polypeptides of different chain

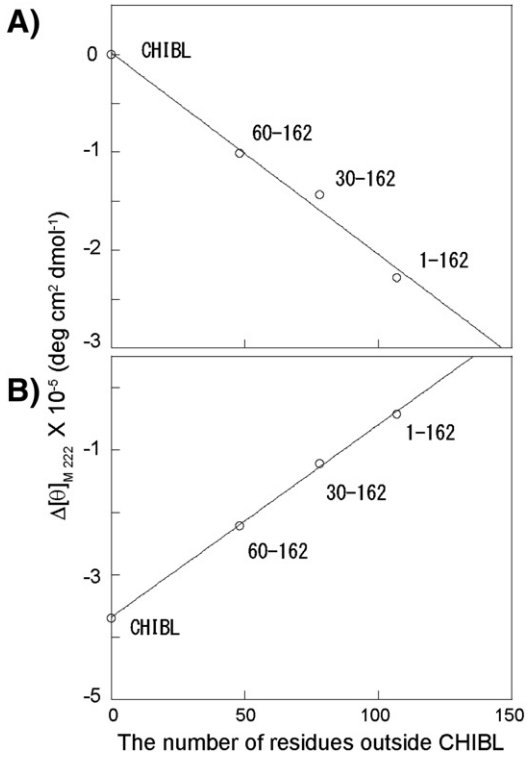

Fig. 5. Dependence of local secondary structures on chain length. (A) The Cl^--induced molar ellipticity change ($\Delta[\theta]_{M\ 222}$) at 25 °C and (B) $\Delta[\theta]_{M\ 222}$ induced by the L103 →P mutation at 25 °C are shown as a function of the number of residues excluding those of CHIBL.

lengths can be made. Fig. 6A and B are the temperature-dependence of molar ellipticity at 222 nm in the absence and presence of Cl^-, respectively. The difference between them, $\Delta[\theta]_{M\ 222}$, (Fig. 6C) was calculated by subtracting the $[\theta]_{M\ 222}$ in the absence of Cl^- (Fig. 6A) from those in the presence of Cl^- (Fig. 6B). Clearly, the cooperativity of the transitions in the presence of 0.1 M Cl^- is largest for 1–162 and decreases with decreasing polypeptide length (Figs. 3 and 6B, C). The $[\theta]_{MRE\ 222}$ for CHIBL exhibits a linear temperature dependence that is independent of Cl^- concentration (Fig. 6A–C).

To confirm that the F- and G-strand regions in 30–162 and 60–162 assume a β-hairpin in the presence of 0.1 M Cl^-, we examined the CD spectra of their L103 → P mutants and found that the replacement reduced the $[\theta]_{MRE\ 222}$ values for 30–162 and 60–162 in the presence and absence of Cl^- (Fig. S4). The difference spectra for all polypeptides and their corresponding L103P mutants when Cl^- is absent are nearly identical and have negative peaks at 222 and 208 nm (Fig. 6D), indicating that L103 is part of an α-helix that is disrupted by the proline substitution. The fractional helicity of CHIBL at 25 °C is possibly ~50% because the helical population of CHIBLΔF is ~50% at 12 °C [15]. If the helical structures in CHIBL are stabilized by non-CHIBL residues, the intensities of the difference spectra should differ according to the chain lengths. Because the difference spectra are all identical (Fig. 6D), the helices present in CHIBL do not appear to be stabilized by non-CHIBL residues. Instead, the observed differences for $[\theta]_M$ at 222 nm for the polypeptides in 0.1 M H_3PO_4 at 25 °C (Fig. 6A) could reflect the CD in the non-CHIBL regions of the polypeptides.

Conversely, the shapes of the difference spectra for the L103-containing polypeptides and their corresponding L103P mutants in 0.1 M Cl^- at 25 °C (Fig. 6E) are remarkably different. Although the difference spectra for CHIBL and CHIBL_L103P in the presence and absence of 0.1 M Cl^- are identical (Fig. 6D, E), the difference spectra of 1–162 and 1–162_L103P in the presence and absence of 0.1 M Cl^- differ significantly with the shape of the spectrum in Fig. 6E indicative of β-hairpin involving L103. The shapes of the difference spectra for the polypeptides in 0.1 M Cl^- change from spectra suggestive of α-helices to one suggestive of a β-hairpin as the length of the polypeptide increases. Fig. 5B shows how the chain length affects the L103 → P-induced $\Delta[\theta]_{M\ 222}$. As observed for the Cl^--induced change, $\Delta[\theta]_{M\ 222}$ depends linearly on chain length. Therefore, as suggested above, the secondary structures in the F- and G-strand regions transition from α-helices to β-hairpins as the chain length increases from 55 residues (CHIBL) to 162 residues (1–162).

3.3. Dependency of molten-globule characters on polypeptide chain length

Besides the local secondary structure in the F- and G-strand region, the global structure is different between the A and C states. The molecule in the A state is compact like as molten globule, whereas in the C state it is expanded and chain-like [9]. Although the sedimentation coefficients shows that the Stokes radii of 1–162, 60–162, and 30–162 are smaller than the value calculated for random-coil polypeptide of the same chain length, experimental error in sedimentation coefficients and uncertainty in partial specific volumes make it difficult to conclude that the truncated mutants are compact.

Other characteristics of the molten globule state are its binding of hydrophobic probe ANS and its substantial fluorescence enhancement [20]. Therefore, we measured the fluorescence spectrum of ANS in the solution of a series of truncated mutants in 0.1 M H_3PO_4 or 0.1 M HCl/KCl at pH 1.7 (Fig. 7). The shortest fragment, CHIBL, slightly enhances the ANS fluorescence intensity and shifts the maximum emission wavelength (λ_{max}) to shorter wavelength both in 0.1 M H_3PO_4 and 0.1 M HCl/KCl (Fig. 7A and B, respectively). The spectra of ANS bound to CHIBL under two conditions are identical, suggesting that the conformation of CHIBL is independent of Cl^- concentration and that the fluorescence properties of ANS do not depend on Cl^- concentration. With increasing the chain length, ANS fluorescence intensities increase and λ_{max} shifted to shorter wavelength (~480 nm in 1–162) in 0.1 M H_3PO_4 (Fig. 7A, C). This may be due to the additional binding sites present in non-CHIBL sequence or may be due to increased affinity of binding sites present in CHIBL region. To clarify this, we expressed a polypeptide chain corresponding to residues 1–87 of C66A/C160A with N-terminal tag. The CD spectrum of 1–87 shows that this fragment does not have remarkable secondary structures (Fig. 3A). The ANS fluorescence spectrum of 1–87 has the maximum at ~500 nm and its intensity is less than that of CHIBL (Fig. 7A, B). Therefore, the chain-length-dependent fluorescence enhancement is not simply due to the additional binding sites in non-CHIBL sequence, but is brought about by the collaboration between CHIBL and non-CHIBL sequences. Furthermore, the enhancement is much more pronounced in 0.1 M HCl/KCl relative to that in 0.1 M H_3PO_4 (Fig. 7A–C), suggesting that the conformational difference between in 0.1 M HCl/KCl and in 0.1 M H_3PO_4 plays an important role in ANS binding and fluorescence enhancement. Clearly, more extensive hydrophobic regions are developed in 0.1 M HCl/KCl. This is similar to the observation that the molten globule formed at acidic pH and high salt concentration shows intense and blue-shifted ANS fluorescence in comparison to the acid unfolded state under low salt conditions at the same pH [21].

4. Discussion

The study reported herein shows that the β-hairpin in the CHIBL sequence in C66A/C160A is stabilized by non-CHIBL residues. This stabilizing effect seems to depend on the chain length in one of two ways as follows. Residues located in the three absent sequences (1–29, 30–59, and 60–87 plus 143–162) may interact specifically with CHIBL residues and contribute additively to the stability of the β- hairpin. In

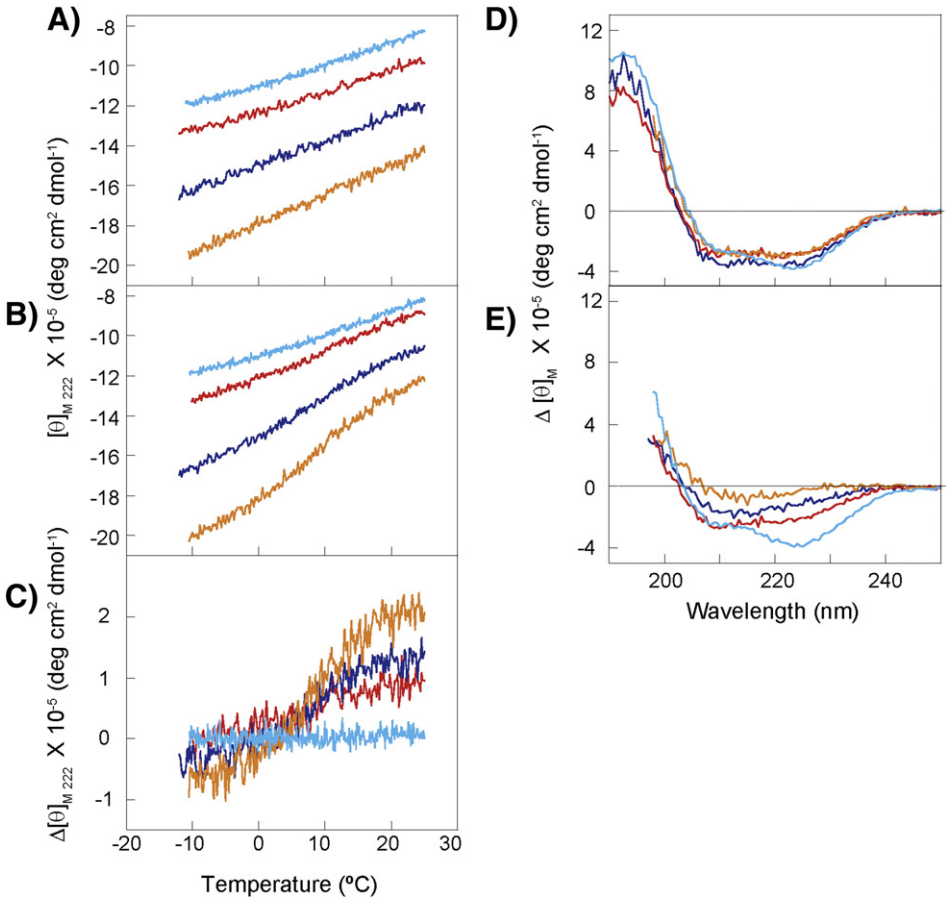

Fig. 6. Temperature dependence of the CD and difference CD spectra. Temperature dependence of the CD spectra for 1–162 (orange), 30–162 (blue), 60–162 (red), and CHIBL (cyan) in (A) 0.1 M H_3PO_4 or (B) 0.1 M HCl/KCl at pH 1.7 and (C) difference between (A) and (B). Difference spectra for the L103-containing polypeptides and their corresponding L103P mutants in (D) 0.1 M H_3PO_4 or (E) 0.1 M HCl/KCl at pH 1.7 and 25 °C. The color coding is the same in the five panels. Note that molar ellipticity values are reported.

the A state (high Cl^- concentration and 25 °C), the molecule is compact, which increases the effective concentrations of the interacting residues, thus stabilizing the β-hairpin. Conversely, the compact globularity may be the result of such specific interactions. However, no ordered structure has been detected in residues 1–87 and 143–162 by hydrogen–deuterium exchange [6] and proline-scanning mutagenesis [8].

Alternatively, the non-CHIBL residues may provide a hydrophobic environment for the β-hairpin in the CHIBL sequence. If a native-like β-hairpin can form in the F- and G-strand region, spatially nearby hydrophobic residues may form hydrophobic patches surrounding the β-hairpin. Conversely, when the F- and G-strand region assumes a non-native α-helix(s), the hydrophobic side chains are spatially dispersed. Therefore, the hydrophobic surface of the β-hairpin would be more readily sequestered from water by stochastic contacts with non-CHIBL hydrophobic residues. To sequester hydrophobic side chains that are widely distributed, many hydrophobic clusters must be made simultaneously, which seems unlikely and suggests that the β-hairpin will more likely be stabilized when an amphiphilic polypeptide is attached to the CHIBL sequence. The probability of stochastic hydrophobic contacts will be greater for a longer chain if the average content of the hydrophobic residues is a constant value throughout the chain. If we define Val, Leu, Ile, Pro, Met, Phe, Tyr, and Trp as hydrophobic residues, then 1–29 and 30–59 contain 10 and 14 hydrophobic residues, respectively. For 60–87 and 143–162, which are present in 60–162, but absent in CHIBL, the number of hydrophobic residues is 16. Thus, the fractional content of hydrophobic residues is 0.34 (10/29), 0.47 (14/30), and 0.33 (16/48) for 1–29, 30–59, and 60–87 plus 143–162, respectively. Although 30–59 contains relatively more hydrophobic residues (0.47), the other regions have similar hydrophobic contents (~0.34). Therefore, as the chain length increases, the absolute number of hydrophobic residues that may contact the hydrophobic surface of the β-hairpin in the CHIBL sequence increases. This is reflected in the chain-length dependence of ANS fluorescence (Fig. 7). With increasing the chain length, ANS fluorescence increases because it is more probable that hydrophobic residues apart on the sequence (such as CHIBL and non-CHIBL residues) make a binding site together. The dependence is more pronounced in 0.1 M HCl/KCl (Fig. 7C). Under such conditions, electrostatic repulsions between positively charged amino acid residues are suppressed so that the polypeptide chain assumes a compact conformation. As a result, the effective concentration of hydrophobic residues becomes high, and ANS binding sites are made easier. In this scenario, the hydrophobic interactions are nonspecific. That the tag does not affect the A-state conformation (Fig. S1) may be a consequence of its low hydrophobic residue content (4 of 20 residues).

The partially folded state of apomyoglobin contains a native-like subdomain including formed A, G, and H helices [22] and both specific [23,24] and nonspecific [23,25] intra-subdomain interactions seem to stabilize its structure. The acid state of α-lactalbumin has a native-like subdomain [26]. A sequence-minimization experiment suggested that nonspecific hydrophobic interactions may be sufficient to stabilize the native-like fold in the subdomain fragment [27]. However, the same authors also showed some specificity in the side-chain packing in the core of the subdomain [28]. For ELG, the subdomain formed by CHIBL sequence contains nonnative structures. Therefore, it is unlikely that native-like intra-subdomain interactions stabilize such nonnative structures. It will be interesting to determine if the interactions between residues located inside and outside the subdomain are specific or

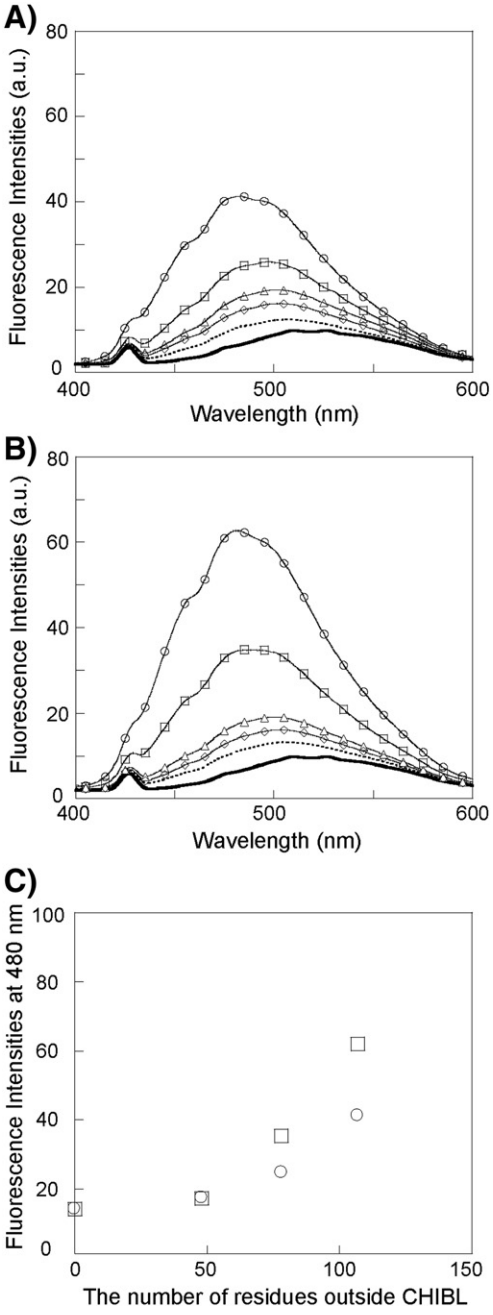

Fig. 7. Fluorescence emission spectra of ANS. The fluorescence emission spectra of ANS with 1–162 (circle), 30–162 (square), 60–162 (triangle), CHIBL (diamond), and 1–87 (dotted line) in (A) 0.1 M H_3PO_4 or (B) 0.1 M HCl/KCl at pH 1.7 and 25 °C. The thick lines represent the spectra of ANS only. (C) The ANS fluorescence intensities at 480 nm in 0.1 M H_3PO_4 (circle) or 0.1 M HCl/KCl (square) are shown as a function of the number of residues excluding those of CHIBL.

nonspecific because the incorrect structure in the subdomain is corrected by such interactions. This question will be addressed in future studies.

5. Conclusion

We used CD spectroscopy to study the α → β transition in partially folded truncated forms of ELG. The α → β transition depends on the length of the polypeptide chain even though ordered structures have not been detected in regions not involved in the α → β transition. Dependence on chain length represents a previously uncharacterized means by which an unstructured polypeptide chain can promote local folding.

Acknowledgments

The authors thank Dr. Seiichi Tsukamoto and Dr. Hideaki Ohtomo for help with the construction of the expression system, protein purification, and CD measurements.

Appendix A. Supplementary data

Supplementary data to this article can be found online at http://dx.doi.org/10.1016/j.bpc.2012.06.002.

References

[1] L. Serrano, The relationship between sequence and structure in elementary folding units, Adv. Protein Chem. 53 (2000) 49–85.
[2] D.L. Minor Jr., P.S. Kim, Context-dependent secondary structure formation of a designed protein sequence, Nature 380 (1996) 730–734.
[3] D. Hamada, S. Segawa, Y. Goto, Non-native alpha-helical intermediate in the refolding of beta-lactoglobulin, a predominantly beta-sheet protein, Nat. Struct. Biol. 3 (1996) 868–873.
[4] K. Fujiwara, M. Arai, A. Shimizu, M. Ikeguchi, K. Kuwajima, S. Sugai, Folding-unfolding equilibrium and kinetics of equine beta-lactoglobulin: equivalence between the equilibrium molten globule state and a burst-phase folding intermediate, Biochemistry 38 (1999) 4455–4463.
[5] J. Li, M. Shinjo, Y. Matsumura, M. Morita, D. Baker, M. Ikeguchi, H. Kihara, An alpha-helical burst in the src SH3 folding pathway, Biochemistry 46 (2007) 5072–5082.
[6] T. Kobayashi, M. Ikeguchi, S. Sugai, Molten globule structure of equine beta-lactoglobulin probed by hydrogen exchange, J. Mol. Biol. 299 (2000) 757–770.
[7] M. Ikeguchi, S. Kato, A. Shimizu, S. Sugai, Molten globule state of equine beta-lactoglobulin, Proteins 27 (1997) 567–575.
[8] K. Nakagawa, A. Tokushima, K. Fujiwara, M. Ikeguchi, Proline scanning mutagenesis reveals non-native fold in the molten globule state of equine beta-lactoglobulin, Biochemistry 45 (2006) 15468–15473.
[9] Y. Yamada, T. Yajima, K. Fujiwara, M. Arai, K. Ito, A. Shimizu, H. Kihara, K. Kuwajima, Y. Amemiya, M. Ikeguchi, Helical and expanded conformation of equine beta-lactoglobulin in the cold-denatured state, J. Mol. Biol. 350 (2005) 338–348.
[10] P.L. Privalov, S.J. Gill, Stability of protein structure and hydrophobic interaction, Adv. Protein Chem. 39 (1988) 191–234.
[11] Y. Yamada, K. Nakagawa, T. Yajima, K. Saito, A. Tokushima, K. Fujiwara, M. Ikeguchi, Structural and thermodynamic consequences of removal of a conserved disulfide bond from equine beta-lactoglobulin, Proteins 63 (2006) 595–602.
[12] Y. Yamada, T. Yajima, S. Tsukamoto, K. Nakagawa, K. Fujiwara, H. Kihara, M. Ikeguchi, Chloride-ion concentration dependence of molecular dimension in the acid-denatured state of equine beta-lactoglobulin, J. Appl. Crystallogr. 40 (2007) S213–S216.
[13] Y. Goto, N. Takahashi, A.L. Fink, Mechanism of acid-induced folding of proteins, Biochemistry 29 (1990) 3480–3488.
[14] K. Nakagawa, Y. Yamada, K. Fujiwara, M. Ikeguchi, Interactions responsible for secondary structure formation during folding of equine beta-lactoglobulin, J. Mol. Biol. 367 (2007) 1205–1214.
[15] M. Yamamoto, K. Nakagawa, K. Fujiwara, A. Shimizu, M. Ikeguchi, A native disulfide stabilizes non-native helical structures in partially folded states of equine beta-lactoglobulin, Biochemistry 50 (2011) 10590–10597.
[16] S.C. Gill, P.H. von Hippel, Calculation of protein extinction coefficients from amino acid sequence data, Anal. Biochem. 182 (1989) 319–326.
[17] P. Schuck, Size-distribution analysis of macromolecules by sedimentation velocity ultracentrifugation and lamm equation modeling, Biophys. J. 78 (2000) 1606–1619.
[18] P.K. Devaraneni, N. Mishra, R. Bhat, Polyol osmolytes stabilize native-like cooperative intermediate state of yeast hexokinase A at low pH, Biochimie 94 (2012) 947–952.
[19] D.K. Wilkins, S.B. Grimshaw, V. Receveur, C.M. Dobson, J.A. Jones, L.J. Smith, Hydrodynamic radii of native and denatured proteins measured by pulse field gradient NMR techniques, Biochemistry 38 (1999) 16424–16431.
[20] G.V. Semisotnov, N.A. Rodionova, O.I. Razgulyaev, V.N. Uversky, A.F. Gripas, R.I. Gilmanshin, Study of the "molten globule" intermediate state in protein folding by a hydrophobic fluorescent probe, Biopolymers 31 (1991) 119–128.
[21] A.L. Fink, L.J. Calciano, Y. Goto, T. Kurotsu, D.R. Palleros, Classification of acid denaturation of proteins: intermediates and unfolded states, Biochemistry 33 (1994) 12504–12511.
[22] D. Eliezer, J. Chung, H.J. Dyson, P.E. Wright, Native and non-native secondary structure and dynamics in the pH 4 intermediate of apomyoglobin, Biochemistry 39 (2000) 2894–2901.
[23] M.S. Kay, R.L. Baldwin, Packing interactions in the apomyglobin folding intermediate, Nat. Struct. Biol. 3 (1996) 439–445.
[24] M.S. Kay, C.H. Ramos, R.L. Baldwin, Specificity of native-like interhelical hydrophobic contacts in the apomyoglobin intermediate, Proc. Natl. Acad. Sci. U. S. A. 96 (1999) 2007–2012.

[25] A.M. Bertagna, D. Barrick, Nonspecific hydrophobic interactions stabilize an equilibrium intermediate of apomyoglobin at a key position within the AGH region, Proc. Natl. Acad. Sci. U. S. A. 101 (2004) 12514–12519.
[26] L.C. Wu, Z.Y. Peng, P.S. Kim, Bipartite structure of the alpha-lactalbumin molten globule, Nat. Struct. Biol. 2 (1995) 281–286.
[27] L.C. Wu, P.S. Kim, Hydrophobic sequence minimization of the alpha-lactalbumin molten globule, Proc. Natl. Acad. Sci. U. S. A. 94 (1997) 14314–14319.
[28] L.C. Wu, P.S. Kim, A specific hydrophobic core in the alpha-lactalbumin molten globule, J. Mol. Biol. 280 (1998) 175–182.